

Received March 26, 2020; reviewed; accepted June 28, 2020

## Evaluation of alkali processing for the recycling of rare earth values from spent fluorescent lamps

Neha Shukla, Himanshu Tanvar, Nikhil Dhawan

Department of Metallurgical and Materials Engineering, Indian Institute of Technology, Roorkee, Uttarakhand, 247667, India

Corresponding author: [ndhawan.fmt@iitr.ac.in](mailto:ndhawan.fmt@iitr.ac.in) (Nikhil Dhawan)

**Abstract:** Phosphor samples collected after crushing and sieving of discarded fluorescent lamps comprise approximately 31 % rare earth elements in the form of  $Y_{1.90}Eu_{0.10}O_3$ ,  $Al_{11}Ce_{0.67}MgO_{19}Tb_{0.33}$ , and  $Al_{10.09}Ba_{0.96}Mg_{0.91}O_{17}:Eu^{2+}$  phase. Direct leaching and mechanical activation assisted leaching are incapable of recovering Ce, Tb values from the  $Al_{11}Ce_{0.67}MgO_{19}Tb_{0.33}$  phase. Heat treatment with NaOH was found successful for dissociation of Ce, Tb phase via substitution of rare-earth ion by  $Na^+$  ion to form rare earth oxide and water-soluble  $NaAlO_2$ . Y, Eu, Ce, and Tb values were recovered from heat-treated mass in a two-step leaching process followed by recovery from the leach solution by oxalic acid precipitation. Over 95 % extraction rate was attained after heat treatment at 400 °C with 150 wt-% NaOH for 1 h. It was found that Y, Eu containing phase does not take part in the heat treatment process whereas the Ce, Tb phase undergoes a solid-state chemical reaction with NaOH via product layer diffusion model with 41.5 kJ/mol activation energy. Approximately 15 g mixed oxide (purity >95 %) of Y (79 %), Eu (7 %), Ce (5 %), and Tb (4 %) could be recovered from 100 units of discarded FLs. Microwave treatment of phosphor and NaOH (50 wt-%) yielded approximately 42 % Y, 100 % Eu, 65 % Ce, and 70 % Tb recovery in just 5 min. Approximately 9 g of REO and 5 g of cerium enriched leach residue were recovered from the microwave route within 5 min and depicted high microwave potential application in the recovery of Ce and Tb values from waste phosphor sample.

**Keywords:** fluorescent lamps, rare earth elements, activation energy, recovery, cerium, terbium

### 1. Introduction

The rare earth elements (REEs) find numerous applications, which include catalysts in the metallurgical and chemical industry, magnets, illuminance phosphor, catalytic converter, X-ray, MRI scanning system, and ceramics (Habashi, 2013). The REE extraction from primary ores (bastnasite, monazite, xenotime, igneous phosphate rocks) comprises of mineral processing, leaching, precipitation, and reduction to metal (Habashi, 2013; Gupta and Krishnamurthy, 2017). The REEs are chemically similar, coexists together with a standard industrial grade of 0.15-3 % (IBM, 2017)]. In the last decade, China dominated the production of REEs, with more than 90 % of global production. The increasing demand and rising instabilities in the production of REEs draw attention towards the recovery from secondary sources (Binnemans et al. 2013, Liu et al., 2019).

The presence of phosphors causes luminescent behavior in fluorescent lamps. In general, mainly five types of RE based phosphors are found in fluorescent lamps: red ( $Y_2O_3:Eu^{3+}$ ), blue ( $BaMgAl_{11}O_{17}:Eu^{2+}$ ) and green ( $LaPO_4:Ce^{3+}, Tb^{3+}, (Gd, Mg)B_5O_{12}:Ce^{3+}, Tb^{3+}, (Ce, Tb)MgAl_{11}O_{19}$ ). Among these, YOX possesses the highest intrinsic value due to significant concentrations of yttrium and europium (~ 20 %), and for lamps containing trichromatic phosphors, the REE oxide concentration is ~ 27.9 % (Binnemans et al., 2013). The REE content of phosphor is approximately 23 % and is significantly higher than the RE ore deposits (Tan et al., 2016; Loy et al., 2017). Therefore, the abundantly available discarded fluorescent lamps (FLs) can be considered a potential RE source. At present, there are limited efforts

for REEs recovery from FL's recycling, which includes mainly hydrometallurgical, pyrometallurgical, and mechanical activation routes. The key findings in the literature for the recycling of FL phosphor are shown in Table 1. Hydrometallurgical studies include extraction of both Y and Eu through leaching and precipitation or solvent extraction routes. The dissolution is favored at a high acid concentration (4 – 5 M) and temperature (75 – 95 °C). However, the direct leaching is ineffective for recovery of Tb and Ce from the green ((Ce,Tb)MgAl<sub>11</sub>O<sub>19</sub>) phosphor due to its inert nature. Pyrometallurgical studies involve heat treatment with flux (NaOH) and are found successful in unlocking the Ce, Tb bearing phases.

Table 1. Key findings in literature for recycling of waste fluorescent lamp phosphor

S. No.	Feed composition	Process conditions	Key results	Reference
1	15.5 % Y, 0.9 % Eu, 0.7 % Ce, 7.7 % Al, 10.3 % Si, 14.6 % Ca, 8.9 % P	Leaching in 4 M HCl for 4 h at 60 °C followed by sintering of residue with NaOH (1:0.5 mass ratio) at 800 °C for 2 h and dissolution of Ce, Tb values in HCl.	94.6 % Y, 99.05 % Eu, 71.45 % Ce, and 76.22 % Tb recovered in solution.	Liu et al., 2014
2	0.3 % Y, 2.6 % Eu, 2.6 % Ce, 1.7 % Tb, 75 % Al	Reductive roasting of phosphor with NaOH (1:2 mass ratio) in presence of 10 % reductive ferrous powder at 700 °C for 3 h. Leaching in 3 M HCl at 70 °C for 1 h.	98.1 % Ce, 99.9 % Eu, 99.3 % Tb, 99.6 % Y recovery.	Liang et., 2016
3	6.8 % Y, 0.4 % Eu, 7.73 % Al, 1.1 % Si, 70.0 % Ca	1. Leaching in 0.5 M HNO <sub>3</sub> for 24 h at 20 °C. 2. Leaching of Y, Eu values in 1 M HNO <sub>3</sub> for 24 h and recovery of Y, Eu via 35 vol% Cyanex 923 in kerosene.	More than 95 % Y, Eu dissolution.	Tunsu et al. 2014, 2016
4	9.7 % Y, 0.7 % Eu, 1.8 % Ce, 0.6 % Tb, 1.7 % La, 8.9 % Al, 24.7 % Si, 20.5 % Ca, 21.1 % P	Leaching of Y, Eu in 2 M HCl at 80 °C for 30 min.	98 % Y, 97 % Eu recovery with an activation energy of 77.49 kJ/mol for Y and 72.75 kJ/mol for Eu.	Eduafo and Mishra, 2018
5	26.4 % Y, 2.2 % Eu, 3.9 % Ce, 2.2 % Tb, 35 % Al	Mechanical activation of phosphor with NaOH (300 wt-% dosage) in a planetary mill for 60 min. Leaching in 2 M H <sub>2</sub> SO <sub>4</sub> for 120 min at 80 °C.	Recovery of 85.0 % Ce and 89.8 % Tb along with total RE recovery of 95 %.	He et al., 2018
6	28.0 % Y, 2.0 % Eu, 3.6 % Ce, 2.1 % Tb, 3 % La, 14.8 % Al	Leaching in 9 % (v/v) H <sub>2</sub> SO <sub>4</sub> solution for 4 h at 70 °C with 10 % (w/v) pulp density.	More than 95 % Y, Eu recovery.	Anand et al., 2019
7	23.1 % Y, 2.5 % Eu, 2.3 % Ce, 1.4 % Tb, 25.0 % Al, 7.3 % Si	Planetary ball milling of phosphor powder for 20 – 30 min followed by leaching in 3 M HNO <sub>3</sub> at 40 °C and RE recovery via precipitation.	Y-Eu oxide recovery with purity more than 98 % and 90 % recovery rate.	Tanvar and Dhawan, 2019

In our previous study, it was found that Ce Tb bearing phases are inert even with rigorous milling (120 min) and leaching (~6 M) conditions (Tanvar and Dhawan, 2019). There are few studies focused on alkali activation with sodium hydroxide to dissolve up to 90 % Ce, Tb values after heat treatment at 500 °C for 2 h and acid dissolution (Liu et al., 2015; He et al., 2018). The mentioned literature studies investigated single-phase or commercial phosphors (CeMgAl<sub>11</sub>O<sub>19</sub>: Tb<sup>3+</sup>), shows dissolution results rather than the extracted RE values and lacks material balance. In this lieu, an attempt is laid to recover the Y, Eu, Ce and Tb values from the massive waste phosphor present in the discarded FLs. Considering the significant presence of Al (~38 %) in the feed and its tendency to form water-soluble NaAlO<sub>2</sub> on thermal treatment with NaOH, the combined process of heat treatment-leaching-precipitation is investigated.

Furthermore, microwave treatment of phosphor waste to recovery Ce and Tb is examined for the first time and shows positive results with a significant reduction in heat treatment duration. The

objectives of this work include (1) Recovery of Ce, Tb, Y, Eu values through heat treatment route, (2) statistical design of experiment incorporating different heat treatment parameters, (3) investigation of underlying reaction kinetics, (4) study the effect of microwaves on heat treatment, and (5) overall mass balance.

## 2. Materials and methods

### 2.1. Material and characterization

The discarded FLs were procured from the institute electric warehouse. The FLs were crushed, and glass, coating powder, and electric switch were separated manually. The phosphor powder was segregated from glass and plastic fraction by sieving below 53  $\mu\text{m}$ . The cut off size was selected based on literature to separate the broken glass from phosphor powder (Eduafo and Mishra, 2018; Tanvar and Dhawan, 2019). The composition analysis was conducted using X-ray fluorescence (XRF), scanning electron microscopy (SEM), Electron Dispersive X-ray technique (EDS), and dissolving in aqua regia for ICP analysis. The evaluation of phases in the sample was carried out using X-ray diffractometer with Cu-K $\alpha$  radiation, 10 - 80  $^\circ$ , step size of 0.02  $^\circ$  and 2  $^\circ$ /min scanning rate.

### 2.2. Methods

#### 2.2.1. Experimental procedure

The procedure followed in this work is presented in Fig. 1. The direct leaching and planetary ball milling assisted leaching in different acids resulted in the Y and Eu dissolution, whereas Ce and Tb report to the leach residue due to the inert nature of the (Ce, Tb)  $\text{MgAl}_{11}\text{O}_{19}$  phase (Tanvar and Dhawan, 2019). Heat treatment of the phosphor sample with NaOH was carried out to dissolve Ce and Tb values from the (Ce, Tb)  $\text{MgAl}_{11}\text{O}_{19}$  phosphor. Heat-treated mass was leached in distilled water for 1 h and water-soluble  $\text{NaAlO}_2$  reports to the leach solution as per Eq. (1) and subsequent leach residue was leached in 0.5 M HCl for 2 h for dissolution of RE values as per Eq. (2) and recovery of RE precipitates using oxalic acid as per Eq. (3).

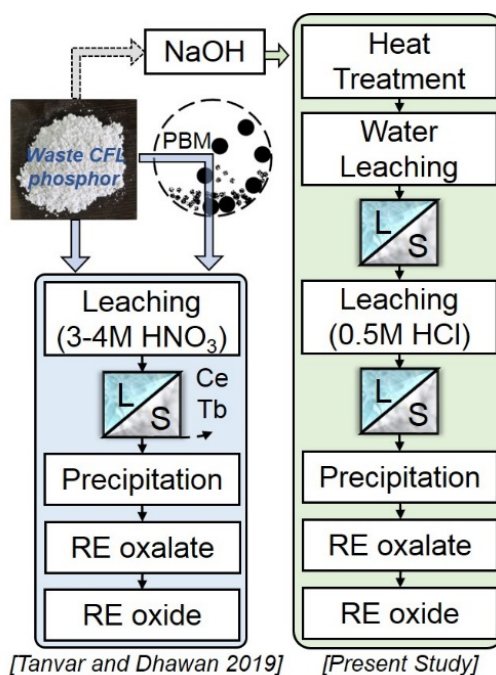
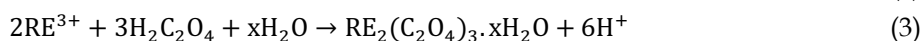
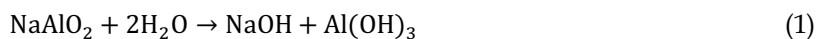


Fig. 1. The experimental procedure used in this work

## 2.2.2. Heat treatment with NaOH

The heat treatment experiments were carried out in a laboratory muffle furnace in a refractory grade crucible with lid. The stoichiometric amount of NaOH was thoroughly mixed with the phosphor sample, followed by heat treatment at a predetermined time and temperature. The optimization of heat treatment parameters was performed using Taguchi's  $L_9$  orthogonal array design (Roy, 1995). The factors included are NaOH dosage, temperature, and time along with the boundary values, as shown in Table 2. The temperature was kept around the melting point of flux (318 °C) as beyond this value effective fusion, i.e., the interaction of feed and flux occurs whereas stoichiometric calculations were carried out to decide the flux dosage. Microwave exposure was attempted in a microwave unit operated at 900 W. The thoroughly mixed phosphor powder and NaOH was placed in a refractory grade crucible inside the microwave unit for a predetermined time (2.5, 5 and 10 min). The temperature attained during the exposure was measured using a metallic thermocouple immediately after the exposure.

Table 2. Factors and boundary conditions for statistical design

Factor	Name	Unit	Levels		
			1	2	3
1	NaOH dosage	%	50	100	150
2	Temperature	°C	240	320	400
3	Time	h	0.5	1	2

## 2.2.3. Leaching and precipitation study

The leaching trials were conducted at 60 °C, with a 5 % pulp density and 900 rpm stirring speed. The filtered residue was oven-dried at 95 °C, and the leach solution was subjected to RE extraction using oxalic acid. Precipitation experiments were performed by adding 0.015 g/cm<sup>3</sup> oxalic acid to the leach solution on continuous stirring for 20 min, and the pH was adjusted to approximately 1 using NH<sub>4</sub>OH or HNO<sub>3</sub> solution (Tanvar and Dhawan, 2019). The recovered precipitates were calcined at 900 °C for 1 h, and corresponding RE extraction was calculated as shown in Eq (4).

$$\%REO \text{ extraction} = (W_{REO} \times \%REE_{REO}) \div (W_{FEED} \times \%REE_{FEED}) \times 100 \quad (4)$$

$W_{FEED}$  and  $W_{REO}$  depict the sample weight applied in leaching and REO weight,  $\%REE_{FEED}$  and  $\%REE_{REO}$  depicts the RE content in feed and REO separated. Similarly, samples were also analyzed using Inductive Coupled Plasma-Mass Spectroscopy (ICP-MS) to calculate the extraction values.

## 3. Results and discussion

### 3.1. Preliminary experiments on RE extraction

The XRF and XRD analysis of feed samples show approximately 31% RE values in the form of  $Y_{1.90}Eu_{0.10}O_3$  (39.9 %),  $Al_{11}Ce_{0.67}MgO_{19}Tb_{0.33}$  (24.6 %) and  $Al_{10.09}Ba_{0.96}Mg_{0.91}O_{17}$ : Eu<sup>2+</sup> (21.4 %) phases. The thermal treatment with NaOH is envisaged to dissociate Ce, Tb rich phosphor phase ( $Al_{11}Ce_{0.67}MgO_{19}Tb_{0.33}$ ), having a distorted magnetoplumbite structure with spinel blocks consisting of Al<sup>3+</sup> and O<sup>2-</sup>, separated by a mirror plane containing O<sup>2-</sup> and large trivalent rare-earth cations such as Ce<sup>3+</sup> and Tb<sup>3+</sup> (Stevens, 1978; Zhang et al., 2001). The crystal structure of the  $Al_{11}Ce_{0.67}MgO_{19}Tb_{0.33}$  phase is shown in Fig. 2. During thermal treatment with sodium-bearing flux, it is expected that Na<sup>+</sup> ion can substitute RE ion in the mirror plane initially because of a similar radius of RE ions with Na<sup>+</sup> ion (Ce<sup>3+</sup> 103.4 pm, Tb<sup>3+</sup> 92.3 pm, Na<sup>+</sup> 102 pm) and RE ions combine with free OH<sup>-</sup> to form H<sub>2</sub>O and REO (Liu et al., 2015). The RE ions combine with free. The grouping of adjacent ions of oxygen, aluminum, and Na<sup>+</sup> leads to NaAlO<sub>2</sub> formation, and Mg<sup>2+</sup> interacts with OH<sup>-</sup> to form MgO and H<sub>2</sub>O. The corresponding chemical reaction is shown in Eq. (5). Furthermore, stoichiometric calculations were performed to select the flux dosage as per Eq. (5) and (6). Ideally, 50 % and 80 % NaOH dosages by weight are required for complete dissociation of  $Al_{11}CeMgO_{19}Tb$  and Al<sub>2</sub>O<sub>3</sub>, respectively. Approximately 12 % or 30 % NaOH dosage is required for complete dissociation of the respective phases in phosphor, i.e., 25 %  $Al_{11}CeMgO_{19}Tb$  or 38 % Al<sub>2</sub>O<sub>3</sub>. 12 % and 30 % NaOH dosage by weight were tested at 400 °C for 30 min;

however, incomplete or limited Ce, Tb dissolution was achieved. Different phases are present in the phosphor sample, and the stoichiometric flux dosage is not sufficient for complete dissociation of the target phase; therefore, flux dosage was increased three times to 100 % (1:1 ratio of feed to flux) by weight. Water leaching was pursued to leach out NaAlO<sub>2</sub> from the heat-treated product, and subsequently, RE values were leached in different acids such as 0.5 M HCl, 0.5 M HNO<sub>3</sub>, and 0.5 M H<sub>2</sub>SO<sub>4</sub> for 2 h and approximately 88 %, 82 % and 73 % RE values were recovered, respectively. Considering that HCl yielded the highest RE extraction; therefore, further leaching experiments were carried out with 0.5 M HCl. To further enhance RE extraction, different heat treatment parameters were optimized by Taguchi L9 statistical design.

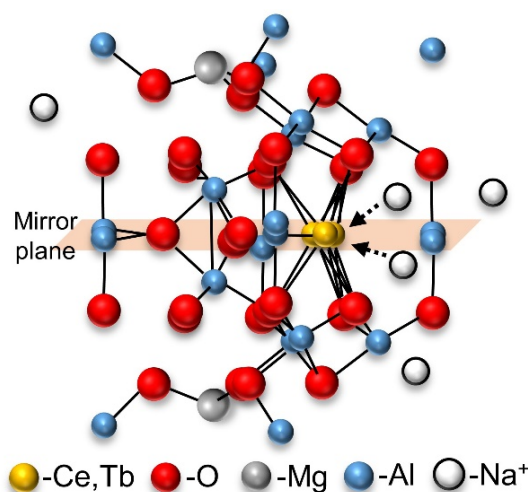
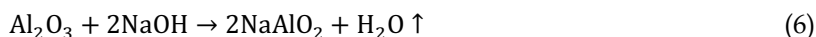
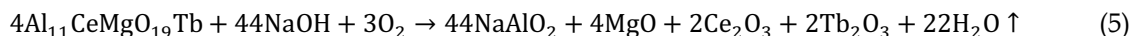


Fig. 2. Crystal structure of Al<sub>11</sub>Ce<sub>0.67</sub>MgO<sub>19</sub>Tb<sub>0.33</sub> phase

### 3.2. Heat treatment with NaOH

The RE extraction corresponding to different Taguchi L9 statistical design experiments run shown in Table 3. It should be noted that experiments were performed in triplets, and the average values are reported here. The parameter effect graphs for mean response and experimental results shown in Fig. 3 and Table 3 depicts that flux dosage and temperature are significant factors, whereas the heat treatment time is an insignificant factor. The P-value for the model was found to be 0.177, 0.196, 0.908 for NaOH dosage, temperature, and time, respectively. Since the p-value is higher than 0.05, which is a prerequisite for a statistically significant model, therefore the model equations are not included. Based on experimental data, weight loss of approximately 2-4 % was observed after heating at 400 °C, whereas at lower temperatures (240, 320 °C), a weight loss of ~1 % was observed. The contour plots for temperature-flux and time-flux are shown in Fig. 4 (a, b). An increase in flux dosage and heat treatment temperature favors the RE extraction. At lower flux dosage and temperature, an ineffective fusion of flux and phosphor occurs, resulting in partial dissolution in the leaching step. RE extraction reached up to 97 % after heat treatment at 400 °C for 1 h with a 150 wt-% flux. As per the results, a high dosage of flux and temperature is required for the highest recovery of RE values, whereas extended heating has less effect on the RE extraction. The XRD analysis of heat-treated products for an experiment run 5, 7, and 9 corresponding to 240, 320, and 400 °C are shown in Fig. 5. With the increase in heat treatment temperature, Al<sub>11</sub>Ce<sub>0.67</sub>MgO<sub>19</sub>Tb<sub>0.33</sub> phase dissociation increases, and NaAlO<sub>2</sub> phase formation starts. It is essential to mention that the XRD spectra of different REEs (Y, Eu, Ce, Tb) are quite similar with a major peak at 2θ value of 29.2 °, and due to presence of Y<sub>2</sub>O<sub>3</sub> in the feed, a further new peak for Tb, Ce oxide was not observed after heat treatment due to overlapping. However, the formation of NaAlO<sub>2</sub> ensured the decomposition of the CAT phosphor phase. The regression plot for experimental and predicted values for a different experimental run, as shown in Fig. 6 and a regression coefficient value

( $R^2$ ) of 0.899, depicts that experimentally determined RE extraction is consistent with model-predicted values.

Table 3. Experimental values for heat treatment with NaOH

Run	NaOH (%)	Temp (°C)	Time (h)	Wt. loss (%)	Extraction (%)
1	50	240	0.5	0.17	61.9
2	50	320	1.0	0.00	54.1
3	50	400	2.0	4.00	83.3
4	100	240	1.0	0.50	77.8
5	100	320	2.0	0.25	76.5
6	100	400	0.5	1.63	88.7
7	150	240	2.0	0.70	76.5
8	150	320	0.5	0.50	87.9
9	150	400	1.0	2.10	97.5
Rank	1	2	3	-	-
p-value	0.177	0.196	0.908	-	-

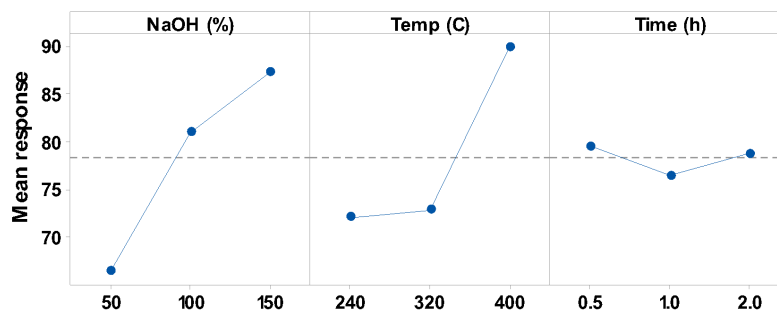


Fig. 3. Main effect plots for the mean response of various factors

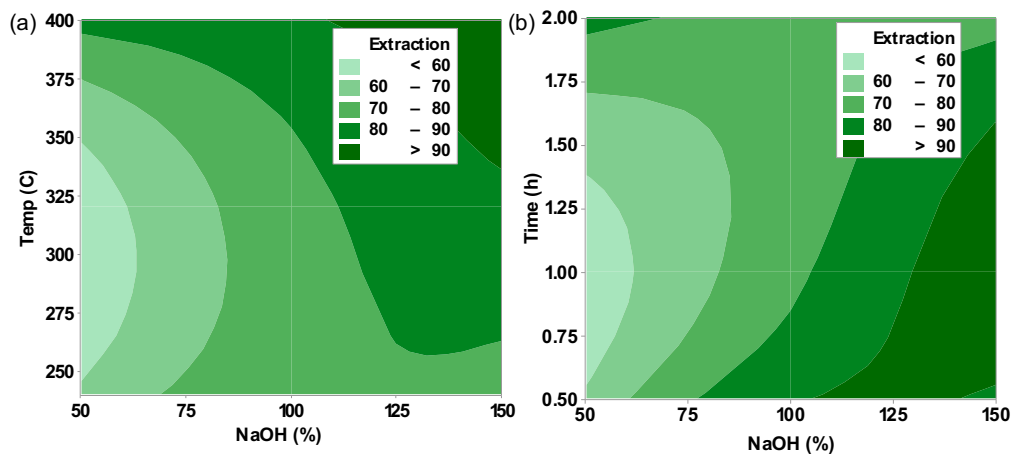


Fig. 4. Contour plots showing the response surfaces for flux dosage with (a) temperature (b) time

### 3.3. Reaction kinetics

Experiments were conducted at 240-400 °C, 30-120 min, with 100 wt-% NaOH dosage to delineate the underlying reaction mechanism. The thermal treatment mechanism is governed either by reaction at the interface or diffusion of reactant and product through the product layer (Antony et al., 2013). The kinetics equations of different mechanisms are mentioned in Eq. (7-9) and involves  $k$  as the reaction rate constant ( $\text{min}^{-1}$ ),  $t$  is roasting time (min), and  $f$  is fraction reacted. Usually interface controlled reaction depends upon the rate at which atoms migrate through the interface into the other crystal. Jandler model is based on parabolic rate law, whereas the Ginstling Brounshtein model describes the parabolic

equation representing the growth of the product layer to the decrease in interface area (Antony et al., 2013).

$$1 - (1 - f)^{\frac{1}{3}} = kt \text{ (Interface controlled reaction)} \quad (7)$$

$$\left(1 - (1 - f)^{\frac{1}{3}}\right)^2 = kt \text{ (Product layer diffusion: Jandler model)} \quad (8)$$

$$1 - \frac{2}{3f} - (1 - f)^{\frac{2}{3}} = kt \text{ (Product layer diffusion: Ginstling Brounshtein model)} \quad (9)$$

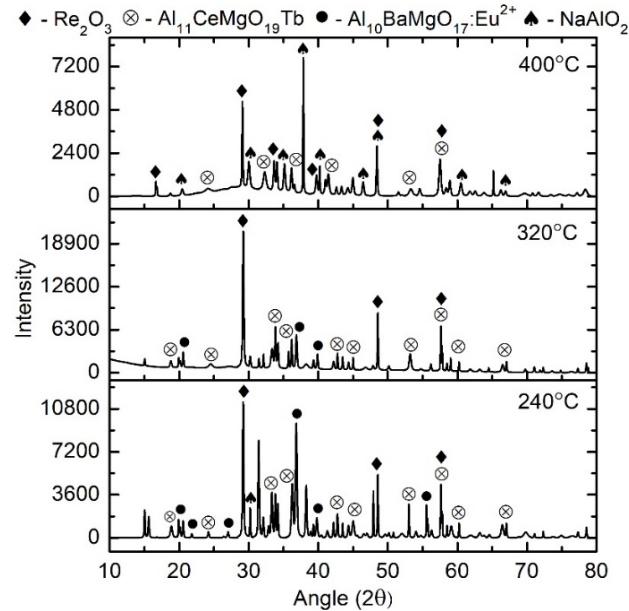


Fig. 5. XRD spectra of heat-treated products at different temperatures

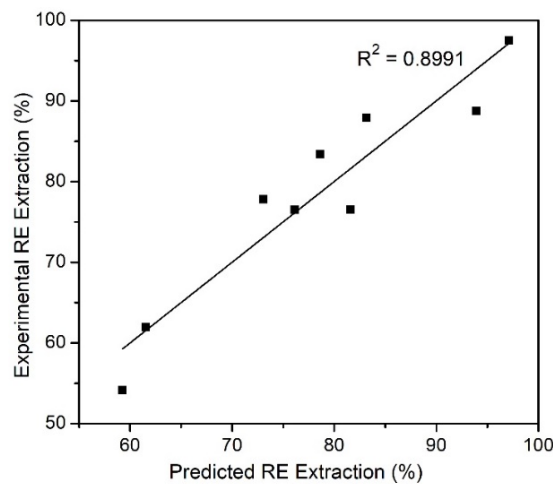


Fig. 6. Regression plot for experimental and predicted values for RE extraction

It was observed that the Y, Eu dissolution saturated in the entire temperature and time range with an average extraction of about 90-95 %. This may be attributed to the fact that Y, Eu bearing phase remains unaffected during heat treatment, whereas the Ce, Tb phase effectively takes part in the fusion process to yield new phases. Therefore, the activation energy calculation was performed for Ce and Tb recovery. The dissolution of Ce and Tb values across different conditions shown in Fig. 7 (a) reveals that higher time and temperature favor the Ce, Tb extraction. Experimental results were verified with standard kinetics models, and the validity of different models at 400 °C is given in Fig. 7 (b). The kinetics data were also analyzed at different temperatures, and the regression coefficient values ( $R^2$ ) were recorded, as shown in Table 4. Based on  $R^2$  values, it was found that the product layer diffusion (Ginstling Brounshtein model) dominated the heat treatment kinetics, and the corresponding activation

energy was determined from the Arrhenius plot as shown in Fig. 7 (c). The reaction rate constant was obtained using the slope of the model equation, and the activation energy was found to be 41.15 kJ/mol.

Table 4. The regression coefficient ( $R^2$ ) values of kinetic models.

Model/Temp	240°C	295°C	345°C	400°C
GB	0.9922	0.8996	0.9528	0.9612
Jandler	0.9926	0.8998	0.9497	0.9598
Interface	0.9659	0.8984	0.9707	0.9659

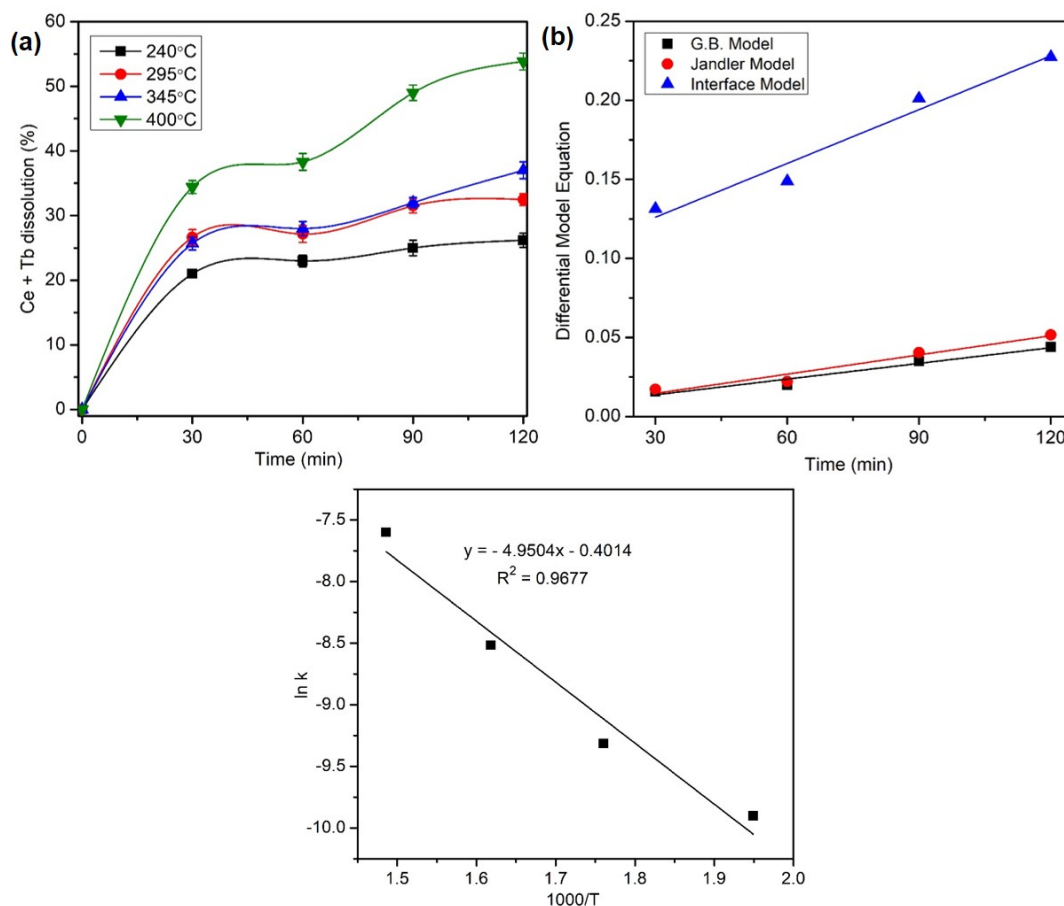


Fig. 7. (a) Ce, Tb dissolution (%) at different time-temperature levels, (b) Validity of different kinetic models at 400 °C as a function of time, (c) Arrhenius plot is corresponding to G.B. model

### 3.4. Product Characterization

The photographs of the sample at a different stage of processing are shown in Fig. 8. Approximately 45 g of phosphor powder was obtained from 100 units of FLs. Heat treatment of phosphor powder with NaOH followed by water leaching removed Al impurity and yielded 38 g of Y, Eu, Ce, Tb rich residue 1. Further leaching of residue in HCl and precipitation produced 15 g of Y, Eu, Ce, Tb oxide with purity more than 95 %. RE extraction reached more than 95 % after heat treatment at 400 °C for 1 h with a 150 wt-% flux followed by water wash and 0.5 M HCl leaching for 2 h. The sample was observed in the sintered and hard form after heat treatment. Leaching and precipitation of heat-treated powder produced a white color RE precipitate, which converted to yellowish powder upon heating at 900 °C.

The color of oxide of Y and Eu being white,  $CeO_2$  yellow, and  $Tb_4O_7$  brown, the off-white color of REO obtained confirms the presence of different RE oxides (Y, Eu, Ce, Tb) (Gupta and Krishnamurthy, 2017). The SEM(EDS) and XRD analysis of REOs extracted at 150 wt-% NaOH, 400 °C, 1 h are shown in Fig. 9 (a) and (b). XRD analysis reveals RE (Y, Eu, Ce, Tb) oxides, and the corresponding micrograph depicted the flakes of size  $\sim 3\text{-}4\ \mu\text{m}$ . EDS values revealed that Y (60 %), Eu (5 %), Ce (4 %), Tb (3 %) are

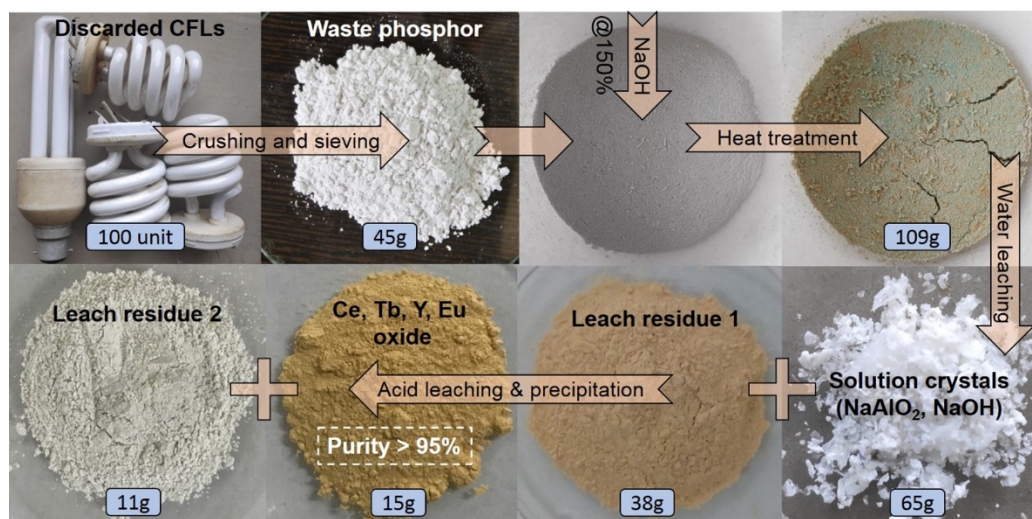


Fig. 8. Sample specimen photographs at a different stage of treatment

the major REEs. To check the purity of the product, 0.5 g of REO was digested in aqua regia solution followed by ICP analysis after 1000 times dilution. The ICP analysis results mentioned in Fig. 9 (c) indicate that the product comprises Y (5878.7 ppb), Eu (509.4 ppb), Ce (389.9 ppb), Tb (279.5 ppb) and Al (368.7 ppb). Compared to mechanical activation assisted leaching route where REO consists of approximately 93 % Y and 5 % Eu, heat treatment with NaOH resulted in the dissolution of Ce and Tb values and combined oxide of Y, Eu, Ce, and Tb was obtained with 79 % Y, 7 % Eu, 5 % Ce, 4 % Tb, and 5 % Al. The XRD spectra and SEM micrograph of leach solution crystals and the leach residue 2 are also shown in Fig. 10. The leach solution crystals consist of  $\text{NaAlO}_2$  and NaOH phase, whereas the acid leaching residue consists of the  $\text{Al}_{11}\text{Ce}_{0.67}\text{MgO}_{19}\text{Tb}_{0.33}$  phase representing unreacted CAT phosphor. Approximately 24 % of the feed by weight reported to the leach residue 2, which mainly consists of Al (~38 %), along with remaining Ce (~6 %), Tb (~3 %) values. Also, the acid leach residue (residue 2) weight fraction was found to increase with a decrease in heat treatment temperature, reflecting incomplete dissociation at a lower temperature.

The work carried investigates the recovery of mixed RE oxide (Y, Eu, Ce, and Tb) from phosphor powder of massive FLs as an alternative REE source. Bench-scale experiments presented in this study can further be optimized at a pilot scale to understand the dissolution behavior at the pilot scale. The material balance indicates that 0.33 Mg of mixed oxide (Y, Eu, Ce, Tb) can be recovered from 1 Mg of phosphor waste. Considering the high value of RE oxides, especially Tb, the recovery process can prove to be economical.

### 3.5. Application of microwaves in heat treatment

Microwave treatment of mineral and waste materials is often found superior to conventional heating for the extraction of various elements (Pickles, 2009). Microwave heating is considered better due to the volumetric heating, which reduces the energy consumption, time required and makes the extraction process energy-efficient (Bobicki et al., 2014; Tanvar et al., 2019). The phosphor sample was mixed with 50 % and 100 % NaOH dosage and treated in a microwave furnace for a different time duration, and approximately 550 °C temperature was attained in all the experiments. The heat-treated mass was further washed in water and leached in HCl for RE recovery. The dissolution of different REE (Y, Eu, Ce, Tb) at different NaOH dosage and exposure duration are shown in Fig. 11 (a) and (b). The microwave exposure time of 5 min was found enough, whereas, higher flux dosage is not recommended. Highest RE extraction was obtained after 5 min exposure with 50 % NaOH, which resulted in the dissolution of approximately 42 % Y, 100 % Eu, 65 % Ce, and 70 % Tb values. The material balance, along with sample specimen photographs, is shown in Figure 11 (c). Approximately 9 g of REO and 5 g of leach residue with major  $\text{CeO}_2$  phase was recovered from the microwave route, compared to the muffle furnace route mass of REO was less due to loss of Y in the form of  $\text{NaYO}_2$ , while the dissolution of Eu, Tb and Ce were

quite high. Significant reduction of heat treatment time from 1 h in a muffle furnace to 5 min in microwave furnace shows that microwave has high potential application in the recovery of Ce and Tb values from waste phosphor sample.

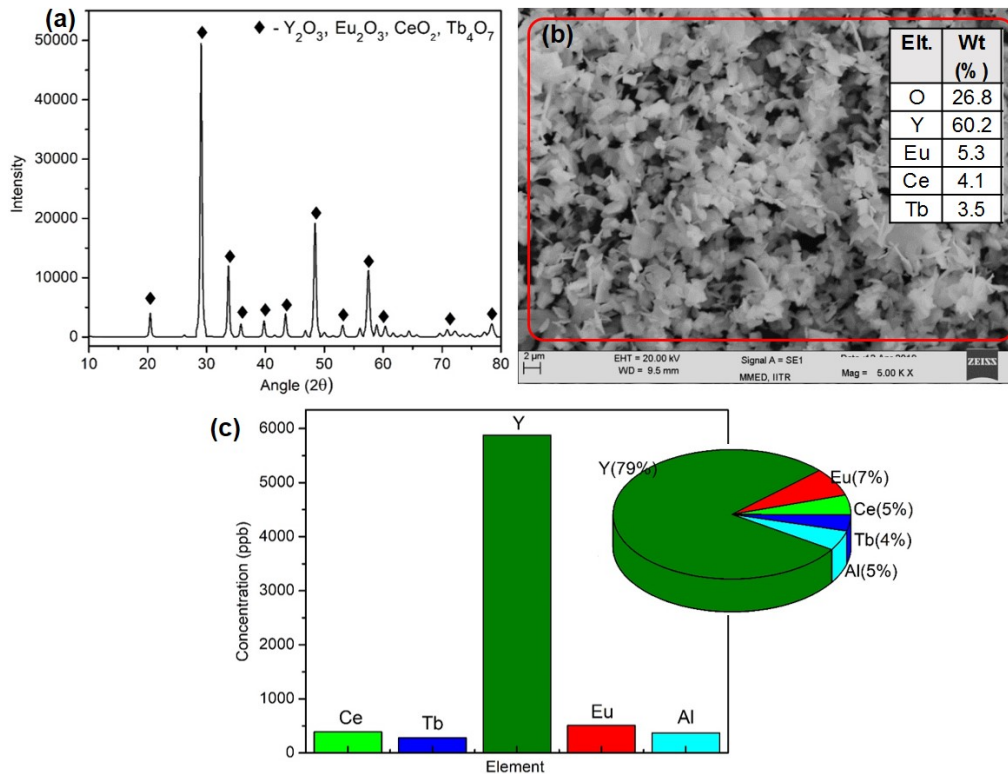


Fig. 9. REO characterization (a) XRD, (b) SEM(EDS), (c) ICP-MS (150 % NaOH, 400 °C, 1 h)

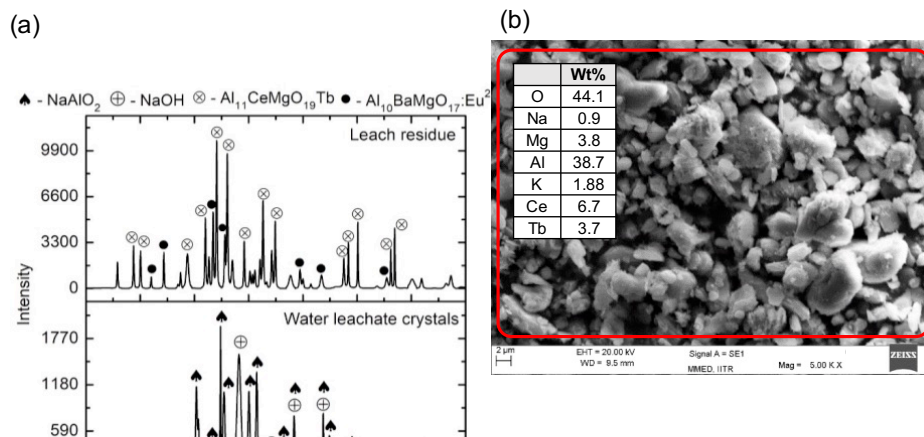


Fig. 10. (a) XRD spectra of water leachate crystals and final leach residue 2, (b) SEM(EDS) analysis of leach residue 2 (150 wt-% NaOH, 400 °C, 1 h)

Fig. 12(a, b) displays the XRD phases of rare earth oxides and leach residues obtained at different microwave exposure time. As per RE dissolution % in Fig. 11(a, b) the XRD patterns of rare earth oxides show  $Tb_2O_3$ ,  $Eu_2O_3$ , and  $Y_2O_3$  phases; because of their chemical similarities, they superimpose each other and are denoted as  $Re_2O_3$  in Fig. 12 (a). The XRD spectra of leach residues in Fig. 12 (b) show that Feed + 50 % NaOH for 5 min of microwave exposure is efficient in dissociating BAM and CMAT phases in the phosphor, while after 10 min and 2.5 min exposure, the formation of  $Ce_{0.27}Y_{0.73}O_{1.635}$  phase and  $Al_2O_3$  phase lead to a lower Y recovery. High temperatures during exposure oxidize  $Ce_2O_3$  to  $CeO_2$  at temperatures above 425–485 °C and lower the recovery of Ce phase (Wenyuan et al., 2006). Furthermore,  $CeO_2$  is often reported to be inert to leaching under mild conditions and require higher acid

concentration ( $> 5 \text{ M}$ ) (Dan et al., 2014; Li et al., 2019).  $\text{NaYSiO}_4$ ,  $\text{AlYO}_3$ ,  $\text{EuAl}_{12}\text{O}_{19}$ ,  $\text{BaAl}_{12}\text{O}_{19}$ ,  $\text{MgAl}_2\text{O}_4$ ,  $\text{CeAlO}_3$ ,  $\text{NaAlSi}_3\text{O}_8$  phases in leach residues of feed + 100 wt-% NaOH show the loss and lower recovery of Y and incomplete decomposition of BAM, CMAT phases.

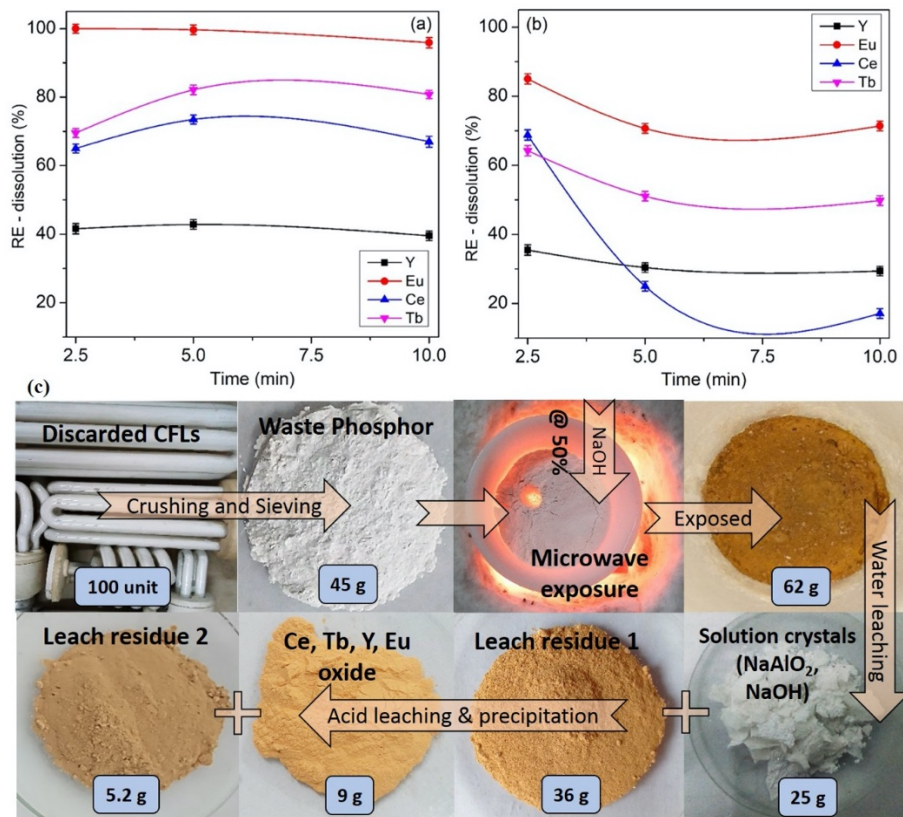


Fig. 11. Effect of microwave exposure on RE dissolution at (a) 50 % NaOH, (b) 100 % NaOH, (c) Material balance and sample specimen photographs (5 min microwave, 50 wt-% NaOH dosage)

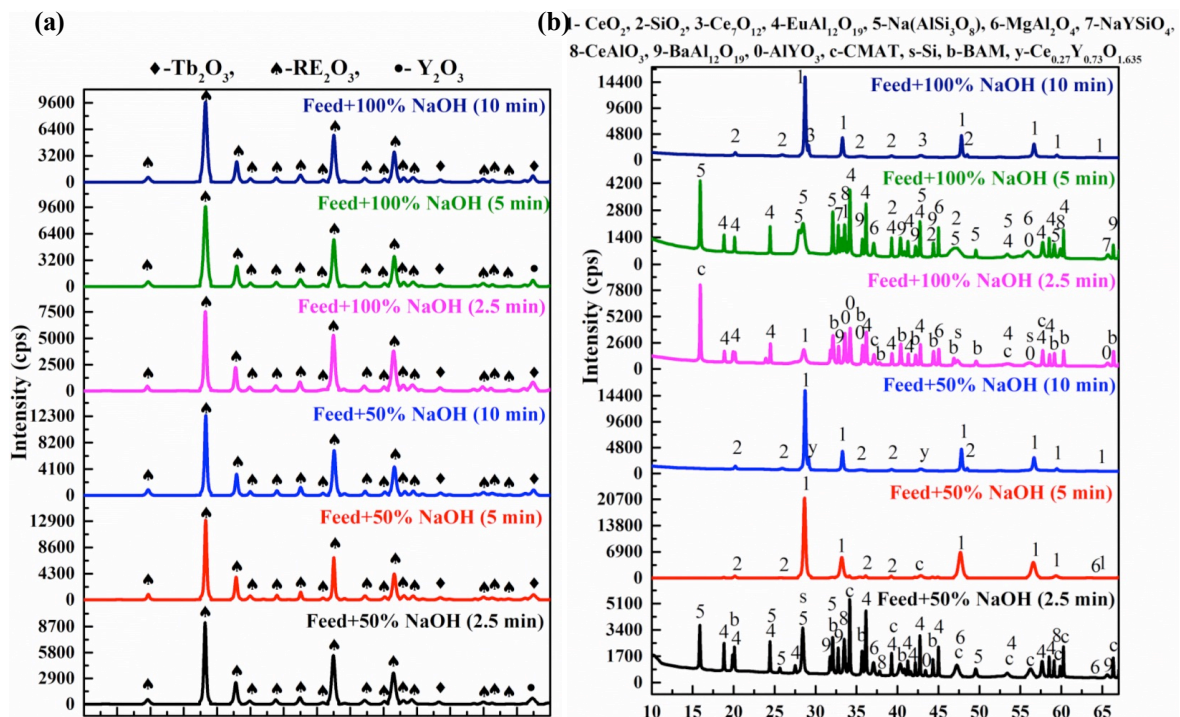


Fig. 12. XRD spectra of (a) rare earth oxides and (b) leach residues obtained from microwave exposure of feed with 50% and 100% NaOH for duration 2.5, 5, and 10 min

#### 4. Conclusions

The waste phosphor sample obtained from crushing and sieving of waste FLs comprise approximately 31% RE values in the form of  $Y_{1.90}Eu_{0.10}O_3$ ,  $Al_{11}Ce_{0.67}MgO_{19}Tb_{0.33}$ , and  $Al_{10.09}Ba_{0.96}Mg_{0.91}O_{17}$ :  $Eu^{2+}$  phases. Heat treatment with NaOH was found successful for dissociation of the  $Al_{11}Ce_{0.67}MgO_{19}Tb_{0.33}$  phosphor phase via the substitution mechanism. Y, Eu, Ce, and Tb values were recovered in a two-step leaching process followed by recovery from the leach solution by precipitation using oxalic acid. RE extraction reached over 95% after heat treatment at 400 °C for 1 h with 150 wt-% flux. The product layer diffusion model governs the heat treatment process with an activation energy of 41.5 kJ/mol. Microwave exposure was found to have a positive impact on the dissociation of the Ce-Tb bearing phase. Microwave exposure for 5 min with 50 wt-% NaOH dosage resulted in the dissolution of 42% Y, 100% Eu, 65% Ce, and 70% Tb values. Microwave exposure resulted in the formation of  $CeY_4O_8$  and  $CeO_2$  phases, which further encapsulated the Y and Ce values. It was determined that approximately 15 g mixed oxide (purity >95%) of Y (79%), Eu (7%), Ce (5%), and Tb (4%) could be recovered from 100 units of discarded FLs. Approximately 9 g of REO and 5 g of cerium enriched leach residue were recovered from the microwave route with a significant reduction of heat treatment time shows that microwave has high potential application in the recovery of Ce and Tb values from waste phosphor sample. The lab-scale results obtained in this study are encouraging and can provide basic guidelines for the scientific community to address and take forward the research.

#### References

- ANAND, A., SINGH, R., SHEIK, A.R., GHOSH, M.K., SANJAY, K., 2019. *Leaching of Rare Earth Metals from Phosphor Coating of Waste Fluorescent Lamps*. Trans. Indian. Inst. Met. 72(3), 623-634.
- ANTONY, M.P., JHA, A., TATHAVADKAR, V., 2013. *Alkali roasting of Indian chromite ores: thermodynamic and kinetic consideration*. Miner. Process. Extr. Metall. 115(2), 71-79.
- BINNEMANS, K., JONES, P.T., BLANPAIN, B., GERVEN, T.V., YANG, Y., WALTON, A., BUCHERT, M., 2013. *Recycling of Rare Earths: A Critical Review*. J. Clean. Prod. 51, 1-22.
- BOBICKI, E.R., LIU, Q., XU, Z., 2014. *Microwave heating of ultramafic nickel ores and mineralogical effects*. Miner. Eng. 58, 22-25.
- DAN, Z., JI, C., DEQIAN, L., 2014. *Separation chemistry and clean technique of cerium (IV): A review*. J. Rare Earths 32, 681-685.
- EDUAFO, P.M., MISHRA, B., 2018. *Leaching Kinetics of Yttrium and Europium Oxides from Waste Phosphor Powder*. J. Sustain. Metall. 4(4), 437-442.
- GUPTA, C.K., Krishnamurthy, N., 2017. *Extractive Metallurgy of Rare Earths*. CRC Press.
- HABASHI, F., 2013. *Extractive metallurgy of rare earths*. Can. Metall. Q. 52(3), 224-233.
- HE, L., JI, W., YIN, Y., SUN, W., 2018. *Study on alkali mechanical activation for recovering rare earth from waste fluorescent lamps*. J. Rare Earth 36, 108-112.
- IBM, Indian Minerals Yearbook 2017 (Part- III: Mineral Reviews) 56th edition: Rare Earths.
- LIANG, Y., LIU, Y., LIN, R., GUO, D., LIAO, C., 2016. *Leaching of rare earth elements from waste lamp phosphor mixtures by reduced alkali fusion followed by acid leaching*. Hydrometallurgy 163, 99-103.
- LIU, H., ZHANG S., PAN D., LIU Y.F., LIU, B., TIAN, J.J., VOLINSKY, A.A., 2015. *Mechanism of  $CeMgAl_{11}O_{19}$ :  $Tb^{3+}$  alkaline fusion with sodium hydroxide*. Rare. Met. 34, 189-194.
- LIU, H., ZHANG, S., PAN, D., TIAN, J., YANG, M., WU, M., VOLINSKY, A.A., 2014. *Rare earth elements recycling from waste phosphor by dual hydrochloric acid dissolution*. J. Hazard. Mater. 272, 96-101.
- LIU, Y.F., ZHANG, S.G., LIU, B., SHEN, H.L., 2019. *An alkaline fusion mechanism for aluminate rare earth phosphor: cation-oxoanion synergies theory*. Rare Met. 38(4), 299-305.
- LI, K., CHEN, J., ZOU, D., LIU, T., LI, D., 2019. *Kinetics of nitric acid leaching of cerium from oxidation roasted Baotou mixed rare earth concentrate*. J. Rare Earths 37, 198-204.
- PICKLES, C.A., 2009. *Microwaves in extractive metallurgy: Part 1 – Review of fundamentals*. Miner. Eng. 22, 1102-1111.
- LOY, S.V., BINNEMANS, K., GERVEN, T.V., 2017. *Recycling of rare earth from lamp phosphor waste: Enhanced dissolution of  $LaPO_4$ :  $Ce^{3+}$ ,  $Tb^{3+}$  by mechanical activation*. J. Clean. Prod. 156, 226-234.
- ROY, R.K., 1995. *A primer on the Taguchi method*. Reinhold, New York.

- STEVENS, A.L.N., 1978.  $Ce^{3+}$  luminescence in hexagonal aluminates containing large divalent or trivalent cations. *J. Electrochem. Soc.* 125(4), 588.
- TAN, Q., DENG, C., LI, J., 2016. *Innovative Application of Mechanical Activation for Rare Earth Elements Recovering: Process Optimization and Mechanism Exploration*. *Scientific Reports* 6, 19961.
- TANVAR, H., DHAWAN, N., 2019. *Recovery of rare earth oxides from discarded compact fluorescent lamps*. *Miner. Eng.* 135, 95–104.
- TANVAR, H., KUMAR, S., DHAWAN, N., 2019. *Microwave Exposure of Discarded Hard Disc Drive Magnets for Recovery of Rare Earth Values*. *JOM* 71(7), 2345-2352.
- TUNSU, C., EKBERG, C., RETEGAN, T., 2014. *Characterization and leaching of real fluorescent lamp waste for the recovery of rare earth metals and mercury*. *Hydrometallurgy* 145, 91–98.
- TUNSU, C., PETRANIKOVA, M., EKBERG, C., RETEGAN, T., 2016. *A hydrometallurgical process for the recovery of rare earth elements from fluorescent lamp waste fractions*. *Sep. Purif. Technol.* 161, 172–186.
- WENYUAN, W., XUE, B., SHUCHEN, S. AND GANFENG, T., 2006. *Study on roasting decomposition of mixed rare earth concentrate in CaO-NaCl-CaCl<sub>2</sub>*. *J Rare Earth*, 24(1), 23-27.
- ZHANG, J., ZHANG, Z., TANG, Z., LIN, Y., 2001. *Mn<sup>2+</sup> luminescence in (Ce, Tb) MgAl<sub>11</sub>O<sub>19</sub> phosphor*. *Mater. Chem. Phys.* 72(1), 81.